Electronic band effects on the spin disorder resistivity of $Gd_4(Co_{1-x}Cu_x)_3$ compounds

Electronic band effects on the spin disorder resistivity of $Gd_4(Co_{1-x}Cu_x)_3$ compounds

T M Seixas[1], M A Salgueiro da Silva[1], O F de Lima[2], J López[2], H F Braun[3] and G Eska[3]

[1] Departamento de Física da Universidade do Porto, Rua do Campo Alegre 687, 4169-007 Porto, Portugal
[2] Instituto de Física Gleb Wataghin, Universidade Estadual de Campinas, 13083-970, Campinas, SP, Brazil
[3] Physikalisches Institut, Universität Bayreuth, D-95440 Bayreuth, Germany

E-mail: tmseixas@fc.up.pt, delima@ifi.unicamp.br and hans.braun@uni-bayreuth.de

Abstract
We present a study of the spin disorder resistivity ($\rho_{m\infty}$) and the electronic specific heat coefficient (γ) in $Gd_4(Co_{1-x}Cu_x)_3$ compounds, with $x = 0.00$, 0.05, 0.10, 0.20 and 0.30. The experimental results show a strongly nonlinear dependence of $\rho_{m\infty}$ on the average de Gennes factor (G_{av}) which, in similar intermetallic compounds, is usually attributed to the existence of spin fluctuations on the Co 3d bands. Values of γ were found around 110 mJ mol^{-1} K^{-2} for the $Gd_4(Co_{1-x}Cu_x)_3$ compounds, much larger than 38.4 mJ mol^{-1} K^{-2} found for the isostructural nonmagnetic Y_4Co_3 compound. Using a novel type of analysis we show that the ratio $\rho_{m\infty}/\gamma^2$ follows a well-defined linear dependence on G_{av}, which is expected when appropriate dependencies with the effective electron mass are taken into account. This indicates that band structure effects, rather than spin fluctuations, could be the main cause for the strong electron scattering and γ enhancement observed in the $Gd_4(Co_{1-x}Cu_x)_3$ compounds. A discussion on relevant features of magnetization and electrical resistivity data, for the same series of compounds, is also presented.

1. Introduction

Rare earth (RE)–transition metal (TM) intermetallics usually present a variety of interesting magnetic properties resulting from the interplay between localized magnetism, typical of RE systems, and itinerant magnetism, which is typical in TM [1]. This is especially exemplified in compounds that contain 3d transition metals, like Co, where 3d(TM)–5d(RE) hybridization and the antiferromagnetic inter-sublattice 4f(RE)–3d(TM) exchange coupling determine the magnetic state of TM atoms. Consequently, these characteristics have a large influence on the magnetic and transport properties of these compounds.

Gd–Co compounds [1, 2] are those that have the highest Curie temperatures among the RE–Co family, due to the direct dependence of the 4f–3d exchange coupling on the spins of the 4f and 3d elements and also due to the fact that Gd is the RE with the highest spin value. When the Co:Gd concentration ratio increases, the itinerant character of the magnetism is enhanced, whereas compounds with a low Co:Gd concentration ratio are expected to exhibit a magnetic behaviour much closer to the 4f localized magnetism typical of rare earths.

The compound Gd_4Co_3 has a relatively low Co:Gd concentration ratio and crystallizes in the hexagonal Ho_4Co_3 type structure [3]. It orders ferrimagnetically below a Curie temperature of $T_C \approx 220$ K [4, 5] with the Co magnetic moments coupled antiparallel to those of Gd. Below $T_{SR} \approx 163$ K [4], and somehow similarly to pure Gd [6], it exhibits a spin-reorientation (SR) process in which the Gd and Co magnetic moments tilt rigidly away from the initial c-axis easy magnetic direction. Recently [7], electrical resistivity as a function of temperature, $\rho(T)$, was measured in several $Gd_4(Co_{1-x}Cu_x)_3$ samples and the SR process was confirmed through a clear anomaly present in $d\rho/dT$. Moreover,

within the magnetically ordered region, $\rho(T)$ showed a strong negative curvature [7], which may indicate the presence of electron scattering by spin fluctuations or a magnon-induced s–d electron scattering typical of d-band magnetic systems.

In this study, we present specific heat measurements for a series of compounds $Gd_4(Co_{1-x}Cu_x)_3$ (x = 0.00, 0.05, 0.10, 0.20 and 0.30) to investigate the role of spin fluctuations and band structure effects on the magnetic contribution to the electrical resistivity. As far as we know, this is the first report on specific heat measurements for this intermetallic system. A combined analysis, involving the de Gennes factor [8] and the electronic specific heat coefficient (γ), indicates that band effects could be the main cause for an observed strong electron scattering and enhanced γ values. A discussion on relevant features of magnetization and electrical resistivity data, for the same series of compounds, is also presented.

2. Experimental details

The $Gd_4(Co_{1-x}Cu_x)_3$ polycrystalline samples were prepared by arc-melting stoichiometric quantities of Gd (3N), Co (4N) and Cu (5N) under a purified argon atmosphere. In order to increase homogeneity, the ingots were remelted several times. Given the very small mass losses, of the order of 0.04%, the initial compositions were assumed to be invariant. The resulting ingots were then encapsulated in quartz tubes under an argon atmosphere and annealed at $600\,^\circ C$ for 2 h, next at $635\,^\circ C$ for 24 h and, finally, at $650\,^\circ C$ for 48 h. X-ray diffraction, measured on the annealed materials, revealed a single phase with the Ho_4Co_3 crystal structure [3].

The average magnetic moment of Co atoms was determined for all samples, through magnetization (M) measurements taken with a Quantum Design MPMS5 SQUID magnetometer, as described in [4] for the case of Gd_4Co_3. Magnetic fields (H) were applied between 0 and 5 T for temperatures in the range of 5–300 K. The saturation magnetic moment per Co atom (μ_{Co}), for all sample compositions, was obtained at the highest field value $H = 5$ T from $M \times H$ curves measured at $T = 5$ K. A conventional dc four-probe technique was used for $\rho(T)$ measurements, in a closed-cycle refrigerator operating from 13 to 300 K. Specific heat measurements were made on samples of $2.5 \times 2.5 \times 1.5$ mm^3, with a Quantum Design PPMS calorimeter that uses a two-relaxation-time technique, and data was always collected during sample cooling. The intensity of the heat pulses was calculated to produce a variation in the temperature bath between 0.5% (at low temperatures) and 2% (at high temperatures) [9]. Experimental errors in all measurements presented here were typically lower than 1%. When required, error bars associated with evaluated parameters will be displayed in the plots of section 3.

3. Results and discussion

Figure 1 shows the specific heat data for the $Gd_4(Co_{1-x}Cu_x)_3$ samples, plotted as C/T versus T^2. For $T \ll \theta_D$, where θ_D is the Debye temperature, one has [10] $C/T = \gamma + \beta T^2$, where γ is the electronic specific heat coefficient and
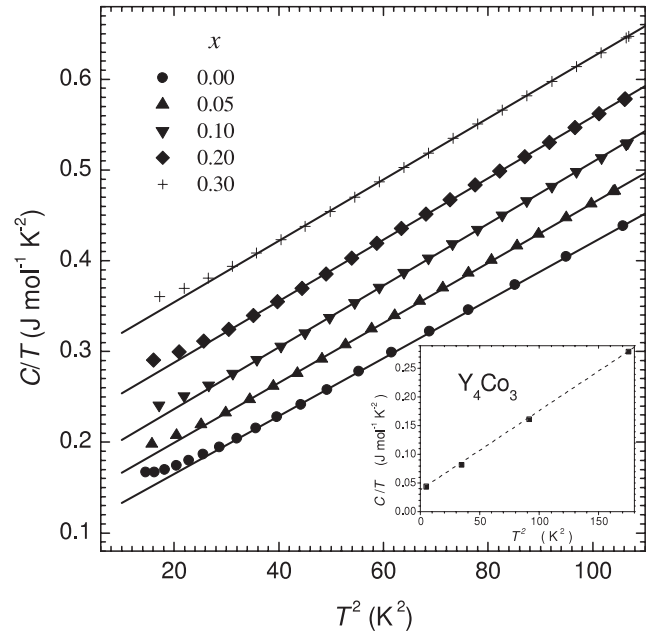
Figure 1. Specific heat data of $Gd_4(Co_{1-x}Cu_x)_3$, plotted as C/T versus T^2, from where each γ value was obtained at the ordinate intersection with the fitted straight line. For $x > 0.0$ a vertical shift of 0.04 J mol^{-1} K^{-2} was applied between the consecutive curves only for the benefit of legibility. The inset shows the same type of plot for a sample of Y_4Co_3.

$\beta = 12\pi^4 NR/(5\theta_D^3)$, where N is the number of atoms per formula unit ($N = 7$ in our case) and $R \approx 8.314$ J mol^{-1} K^{-1} is the ideal gas constant. Therefore, from the slopes of the fitted straight lines in figure 1, we found $\theta_D = 164.3$, 161.2, 160.0, 160.4 and 160.5 K (uncertainty of ± 0.5 K), respectively for x = 0.0, 0.05, 0.10, 0.20 and 0.30. In that same order, the point where each fitted straight line intercepts the vertical axis ($T = 0$) gives γ = 110.0, 98.0, 95.0, 107.0 and 133.0 mJ mol^{-1} K^{-2} (uncertainty of ± 0.5 mJ mol^{-1} K^{-2}). Notice that for $x > 0.0$ a vertical shift of 0.04 J mol^{-1} K^{-2} was applied between the consecutive curves for the benefit of legibility. The inset of figure 1 shows the same type of plot, from where $\gamma = 38.4 \pm 0.8$ mJ mol^{-1} K^{-2} was determined for the sample of Y_4Co_3.

The magnetic contribution to the electrical resistivity for all samples was calculated using the relation $\rho_m(T) = \rho(T) - \rho_{ph}(T) - \rho_0$, where ρ_0 is the residual resistivity and ρ_{ph} is the electron–phonon scattering contribution given by the Bloch–Grüneisen model [11]. Although the obtained θ_D values look very similar, the ρ_{ph} contribution was calculated and subtracted for each composition of $Gd_4(Co_{1-x}Cu_x)_3$. Figure 2 shows plots of $\rho_m(T)$ for all samples, obtained from the previously reported [7] $\rho(T)$ data. For $T > T_C$ in the samples with x = 0.00, 0.05, 0.10 and 0.30 and $T > T_{C1}$ in the sample with $x = 0.20$, a clear plateau appears, associated with a linear dependence of ρ_{ph} in the paramagnetic region. T_C decreases slightly from 220 to around 215 K when the Cu content increases from $x = 0.00$ to 0.10, consistent with a dilution of Co magnetic atoms which can couple ferrimagnetically to Gd. For the sample with $x = 0.20$ a mixed ferrimagnetic phase
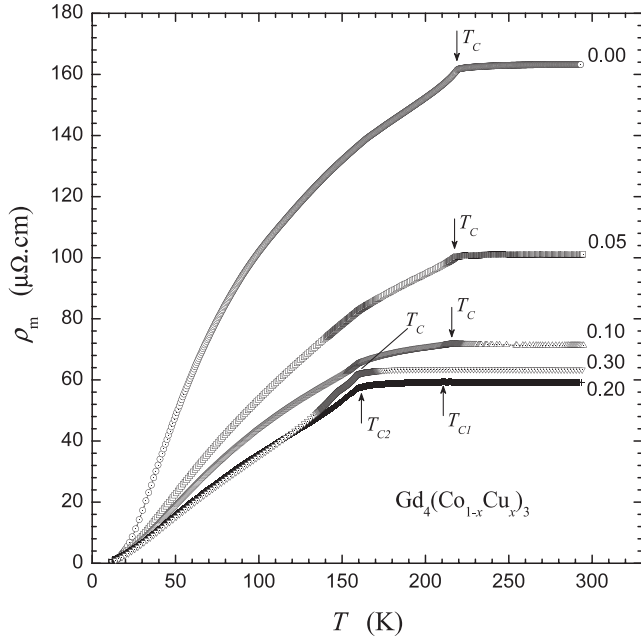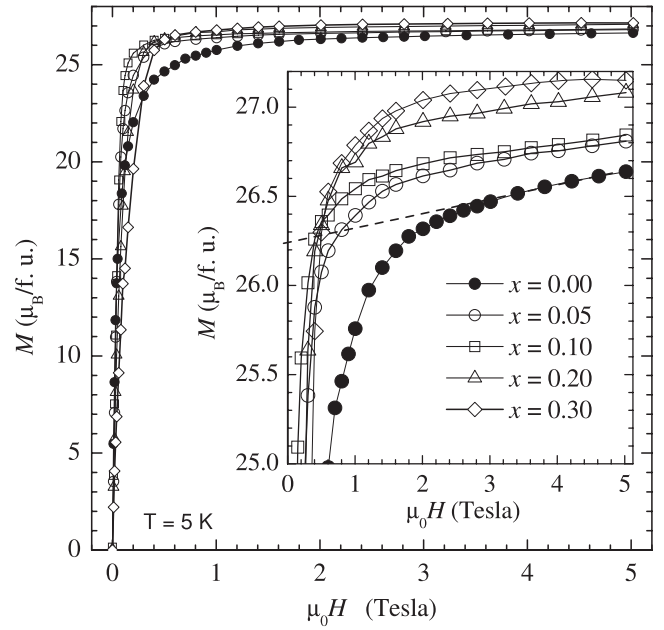
Figure 2. $\rho_m(T)$ is the magnetic contribution to the electrical resistivity, $\rho(T)$, obtained from previously reported data [7]. The numbers to the right of each curve are the sample's x values. A plateau is seen in the paramagnetic region above T_C and T_{C1} (for $x = 0.20$). Below T_C and T_{C2} (for $x = 0.20$) a ferrimagnetic order is established. For $T_{C2} < T < T_{C1}$ a mixed ferrimagnetic phase occurs in sample $x = 0.20$.

Figure 3. Isothermal magnetization curves measured at $T = 5$ K. The saturation magnetic moment (M_S) per formula unit (f.u.) was obtained at the point where an extrapolation of the high field linear part of the curve crosses the vertical axis, as shown in the inset for $x = 0.0$.

occurs between T_{C1} and T_{C2} [7]. This can be attributed to a partial order–disorder transition of the Gd magnetic moments, which goes gradually from a ferrimagnetic phase (for $T < T_{C2}$) to a paramagnetic phase (for $T > T_{C1} = T_C \approx$ 211 K). Since Cu substitutes continuously for Co as x varies in $Gd_4(Co_{1-x}Cu_x)_3$, possibly there will be a range of x values around $x = 0.2$ that exhibits the observed mixed ferrimagnetic phase. For $x = 0.30$ a strong decrease of T_C (162 K) is observed, with no occurrence of mixed phase.

Figure 3 shows isothermal magnetization curves ($M \times H$) measured at a fixed $T = 5$ K. The saturation magnetic moment (M_S) per formula unit (f.u.) was obtained at the point where an extrapolation of the high field linear part of an $M \times H$ curve crosses the vertical axis, as exemplified for $x = 0.0$ in the inset of figure 3. Assuming that each Gd ion carries a magnetic moment of 7 Bohr magnetons (μ_B), then $M_S = [28 - 3(1 - x)\mu_{Co}(x)]\ \mu_B/\text{f.u.}$, where $\mu_{Co}(x)$ is the composition-dependent saturation moment of each Co ion.

The spin disorder resistivity ($\rho_{m\infty}$) is taken as the saturation value of $\rho_m(T)$ at high temperatures (plateau value) for $T > T_C$ in figure 2. Figure 4 shows the compositional dependencies of $\rho_{m\infty}$ (left axis) and μ_{Co} (right axis). It can be observed that the replacement of Co by Cu produces a large and almost exponential decrease of $\rho_{m\infty}$ with x. An exponential decrease is also evident in $\mu_{Co}(x)$, which may be attributed to a strong dependence of the Co magnetic moment on the number of local Co neighbouring atoms. The dashed lines in figure 4 represent the fitted exponential functions $\rho_{m\infty}(x) = \rho_{m\infty}(0)$
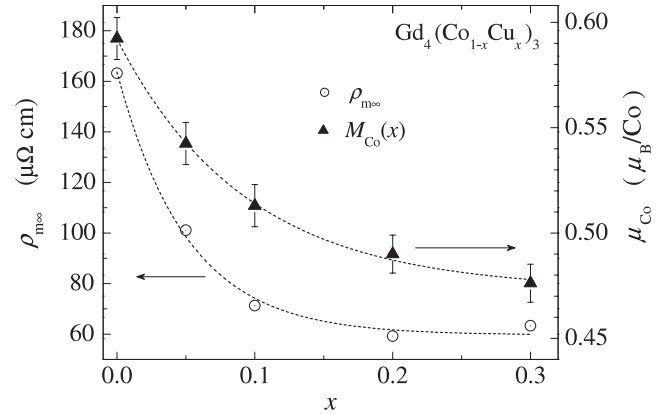
Figure 4. Compositional dependence of the spin disorder resistivity $\rho_{m\infty}(x)$ (left axis) and saturation magnetic moment per Co atom $\mu_{Co}(x)$ (right axis). The dashed lines represent exponential curve fits to the data (see text). Error bars for $\rho_{m\infty}$ are smaller than the data symbol sizes.

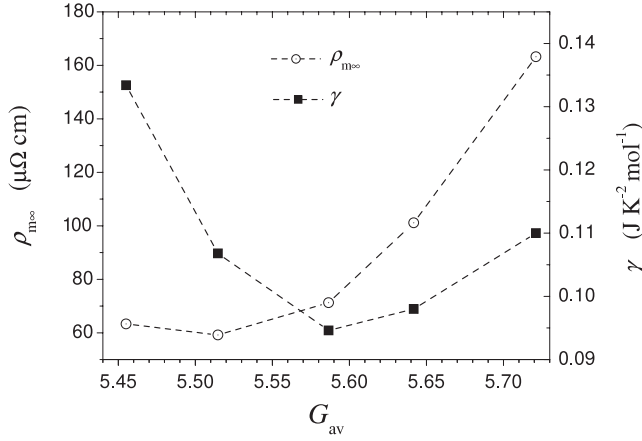$+ \Delta\rho_{m\infty}(x)$, $\mu_{Co}(x) = \mu_{Co}(0) + \Delta\mu_{Co}(x)$, with

$$\Delta\rho_{m\infty}(x) = -104\left[1 - \exp\left(-\frac{x}{0.051}\right)\right] \quad (\mu\Omega\ \text{cm}) \quad (1a)$$

$$\Delta\mu_{Co}(x) = -0.119\left[1 - \exp\left(-\frac{x}{0.094}\right)\right] \quad (\mu_B/\text{Co}) \quad (1b)$$

and $\rho_{m\infty}(0) \approx 164\ \mu\Omega$ cm, $\mu_{Co}(0) = 0.592\ \mu_B/\text{Co}$.

For a system consisting of a single species of localized magnetic moments, the following expression holds [12, 13]:

$$\rho_{m\infty} = \frac{3\pi N}{2\hbar e^2}\frac{m^*}{\varepsilon_F}|\Gamma|^2 G, \quad (2)$$

Figure 5. Dependence of the spin disorder resistivity (left axis) and electronic specific heat coefficient (right axis) with average de Gennes factor G_{av}. Error bars for $\rho_{m\infty}$ and γ are smaller than the data symbol sizes. The dashed lines are only guides to the eyes.
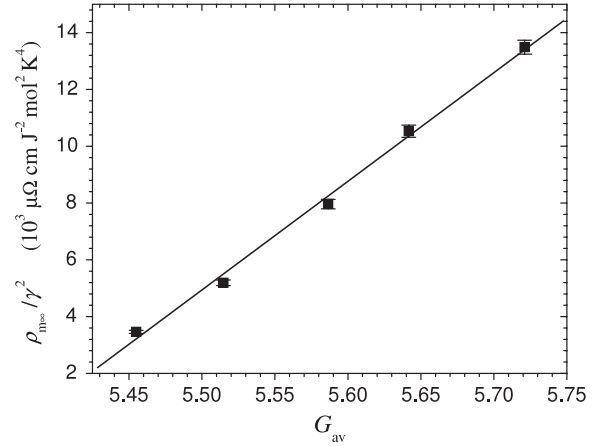
Figure 6. Dependence of $\rho_{m\infty}/\gamma^2$ with the average de Gennes factor in the $Gd_4(Co_{1-x}Cu_x)_3$ samples. The solid line represents a linear fit to the data. Most of the data points have error bars comparable to their symbol's size.

where N is the atomic concentration, m^* is the effective electron mass, ε_F is the Fermi energy, Γ is a parameter describing the interaction between conduction and localized electrons, $G = (g-1)^2 J(J+1)$ is the de Gennes factor, g is the Landé factor and J is the total angular momentum. Since the effective magnetic moment is given by $\mu_{eff} = \mu_B g[J(J+1)]^{1/2}$, it can be shown that

$$\frac{1}{\rho_{m\infty}} \frac{d\rho_{m\infty}}{dx} = 2\left(\frac{1}{\mu_{eff}} \frac{d\mu_{eff}}{dx}\right). \qquad (3)$$

In the derivation of the last equation it was assumed that the compositional dependence of $\rho_{m\infty}(x)$ is linked exclusively to $\mu_{eff}(x)$. If both properties show an exponential decrease, then equation (3) predicts a ratio of 2 between the decay constants of $\rho_{m\infty}(x)$ and $\mu_{eff}(x)$. A ratio of 1.84 was calculated from our $\Delta\rho_{m\infty}(x)$ and $\Delta\mu_{Co}(x)$ data, using the fitted equations written in (1). Assuming that $\Delta\mu_{eff}(x)$ follows the same exponential trend as $\Delta\mu_{Co}(x)$, this result is in good agreement with the model represented by equation (3), thus clearly stressing the important role of the Co 3d electrons on the magnetic scattering observed in the $Gd_4(Co_{1-x}Cu_x)_3$ system.

In order to further analyse the variation of the spin disorder resistivity, we will proceed by investigating its correlation with the average de Gennes factor (G_{av}) in our series of samples. In the case of $Gd_4(Co_{1-x}Cu_x)_3$, in which two magnetic species (Gd, Co) are present, G can be properly averaged by taking into account the respective concentrations ($c_{Gd} = 4/7$, $c_{Co} = 3(1-x)/7$), Landé factors ($g_{Gd} = g_{Co} = 2$) and angular momenta ($J_{Gd} = 7/2$, $J_{Co} = \mu_{Co}/(g_{Co}\mu_B)$). It can be demonstrated that [14]

$$G_{av} = c_{Gd}^2(g_{Gd}-1)^2 J_{Gd}(J_{Gd}+1) + c_{Co}^2(g_{Co}-1)^2$$
$$\times J_{Co}(J_{Co}+1) + 2c_{Gd}c_{Co}(g_{Gd}-1)(g_{Co}-1)J_{Gd}J_{Co}. \quad (4)$$

As shown in figure 5 (left axis), $\rho_{m\infty}$ has a strongly nonlinear dependence on G_{av} for the $Gd_4(Co_{1-x}Cu_x)_3$ samples. Usually, in 4f–nd intermetallics, such nonlinear dependence is attributed to spin fluctuations in the nd band

enhanced by thermal disorder of the 4f magnetic moments. For instance, in the case of Gd_3Co it has been proposed [15] that the enhancement of spin fluctuations by the 4f–3d exchange coupling was responsible for the observed anomalously large values (109–170 mJ mol^{-1} K^{-2}) of γ in this compound, compared to the case of the isostructural nonmagnetic Y_3Co compound (14 mJ mol^{-1} K^{-2}). At first sight such an interpretation seems to be consistent with our present results, which show also large values of γ (see figure 5, right axis) with respect to the isostructural nonmagnetic Y_4Co_3 compound ($\gamma \approx 38.4$ mJ mol^{-1} K^{-2}). This would require γ being an increasing function of the de Gennes factor, as suggested in [15]. However, as seen in figure 5, this is clearly not verified in our case, since γ does not even change monotonically with G_{av}. Therefore, we conclude that the large γ enhancement in the present compounds cannot be ascribed to spin fluctuations, being possibly caused by band structure effects involving only electron–phonon or electron–magnon couplings. As will be shown in the following, the latter hypothesis is very well corroborated by our data.

It is important to notice that, besides the dependence on the de Gennes factor, $\rho_{m\infty}$ also depends on electron band parameters that may change with sample composition. More specifically, and independently of the particular electron band model to be considered, one has [11] $\varepsilon_F \propto (m^*)^{-1}$ and thus, from equation (2), $\rho_{m\infty} \propto (m^*)^2$. Moreover, the variation of the effective electron mass across the $Gd_4(Co_{1-x}Cu_x)_3$ compounds can be inferred from the corresponding variation of the electronic specific heat coefficient, since $\gamma \propto m^*$ [11]. Hence, based on these hypotheses, the quantity $\rho_{m\infty}/\gamma^2$ should be practically independent of the electronic band structure and is expected to scale linearly with G_{av}. Effectively, as shown in figure 6, $\rho_{m\infty}/\gamma^2$ exhibits a well-defined linear dependence on G_{av}, represented by the solid line fitted to the data (regression coefficient = 0.997). This result gives strong support to the relevance of band structure effects on our $\rho_{m\infty}(x)$ data. We would like to emphasize that the important result just presented above is very robust, since it was derived from the combination

of experimental data for two independent properties, specific heat and electrical resistivity, measured in the same samples.

The observed electron mass enhancement can be described using the relations

$$m^*(x, T) = m_b^*(x) [1 + \lambda(x, T)], \quad (5a)$$

$$\gamma(x, T) = \frac{m^*(x, T)}{m_b^*(x)} \gamma_b(x) = \gamma_b(x) [1 + \lambda(x, T)], \quad (5b)$$

where $m_b^*(x)$ and $\gamma_b(x)$ are the composition-dependent effective mass and specific heat coefficient, respectively, derived from band structure and $\lambda(x, T)$ is the composition- and temperature-dependent mass enhancement factor which incorporates the effects of the interactions between conduction electrons and low energy excitations such as phonons and magnons. It should be noticed that, in general, mass enhancement effects by low-lying excitations involve thermal factors that may lead to a temperature dependence of λ.

In the preceding analysis, the low temperature value $\gamma(x, 0)$ has provided an excellent correlation with the high temperature spin disorder resistivity. This indicates that, for temperatures up to the maximum of $T_C(x)$, we have either (a) $\lambda(x, T) \ll 1$ or (b) $\lambda(x, T) = A(x)B(T)$, where $A(x)$ and $B(T)$ are such that $(\partial\lambda/\partial x) \gg (\partial\lambda/\partial T)$ or, equivalently, $(\mathrm{d}\ln A/\mathrm{d}x) \gg (\mathrm{d}\ln B/\mathrm{d}T)$. In case (a), $m^*(x) \approx m_b^*(x)$ and the mass enhancement is due essentially to band structure. In case (b), the compositional dependence of the mass enhancement factor would be stronger than its temperature dependence in order to ensure that $\gamma(x', 0)/\gamma(x, 0) \approx \gamma(x', T_C(x'))/\gamma(x, T_C(x))$ for $x' \neq x$. In either case, band structure changes with composition have to be considered as the main cause for the large mass enhancement effect observed in the present compounds and its role on electron scattering. The effects of electron–phonon and electron–magnon couplings represent minor contributions to the observed mass enhancement.

Different mechanisms could be responsible for a compositional dependence of the electronic band structure. For instance, the dilution of Co by Cu in the $Gd_4(Co_{1-x}Cu_x)_3$ compounds is expected to induce changes in the 3d band structure, which is generally characterized by a high and peaked density of states. This may occur directly through changes of the Fermi level, caused by the filling of 3d band states with Cu-originated electrons. Finally, it is also possible to invoke changes in the lattice parameters and local disorder effects, associated with the substitution of Co by Cu, as concurrent mechanisms for band structure changes.

4. Conclusion

Magnetization, electrical resistivity and specific heat measurements were presented and analysed for a series of $Gd_4(Co_{1-x}Cu_x)_3$ samples with $x = 0.00, 0.05, 0.10, 0.20$ and 0.30. The spin disorder resistivity ($\rho_{m\infty}$) as well as the saturation magnetic moment of cobalt atoms (μ_{Co}) have shown a similar exponential decrease as x increases, with Co atoms being gradually substituted by Cu atoms. The important role

of the Co 3d electrons in the exchange interaction with the Gd 4f electrons was evidenced by the calculated ratio of 1.84 between the decay constants of the exponential laws fitted to the $\rho_{m\infty}(x)$ and $\mu_{Co}(x)$ data, in good agreement with the ratio of 2 predicted by equation (3).

The electronic specific heat coefficient (γ), obtained from C/T versus T^2 plots, present values around 110 mJ mol^{-1} K^{-2} for the $Gd_4(Co_{1-x}Cu_x)_3$ compounds, much larger than the value of 38.4 mJ mol^{-1} K^{-2} observed for the isostructural non-magnetic Y_4Co_3 compound. It was also found that both γ and $\rho_{m\infty}$ exhibit a strongly nonlinear dependence on the average de Gennes factor (G_{av}), while the ratio $\rho_{m\infty}/\gamma^2$ presented a well-defined linear dependence on G_{av}. Since $\rho_{m\infty} \propto (m^*)^2$ and $\gamma \propto m^*$, where m^* is the effective electron mass, we conclude that band structure effects, rather than spin fluctuations, could be the main cause for the strong electron scattering and γ enhancement observed in the $Gd_4(Co_{1-x}Cu_x)_3$ compounds. We expect that other 4f–nd compounds might also show a similar behaviour; therefore more experimental work would be very useful in this area.

References

[1] Liu J P, de Boer F R, de Chatel P F, Coehoorn R and Buschow K H J 1994 *J. Magn. Magn. Mater.* **132** 159
[2] Duc N H, Hien T D, Givord D, Franse J J M and de Boer F R 1993 *J. Magn. Magn. Mater.* **124** 305–11
[3] Lemaire R, Schweizer J and Yakinthos J 1969 *Acta Crystallogr.* B **25** 710–3
[4] Seixas T M, Machado da Silva J M, Papageorgiou T P, Braun H F and Eska G 2004 *Physica* B **353** 34–40
[5] Berthet-Colominas C, Laforest J, Lemaire R, Pauthenet R and Schweizer J 1968 *Cobalt* **39** 97
    Gratz E, Sechovsky V, Wohlfarth E P and Kirchmayr H R 1980 *J. Phys. F: Met. Phys.* **10** 2819
[6] Kaul S N and Srinath S 2000 *Phys. Rev.* B **62** 1114
[7] Seixas T M, Machado da Silva J M, Braun H F and Eska G 2008 *J. Appl. Phys.* **103** 07B720–3
[8] Jensen J and Mackintosh A R 1991 *Rare Earth Magnetism* (Oxford: Clarendon)
[9] López J, de Lima O F, Lisboa-Filho P N and Araujo-Moreira F M 2002 *Phys. Rev.* B **66** 214402
[10] Kittel C 1986 *Introduction to Solid State Physics* 6th edn (New York: Wiley)
[11] Blatt F J 1968 *Physics of Electronic Conduction in Solids* (New York: McGraw-Hill)
[12] Dekker A J 1965 *J. Appl. Phys.* **36** 906
[13] Coqblin B 1977 *The Electronic Structure of Rare-Earth Metals and Alloys: the Magnetic Heavy Rare-Earths* (London: Academic)
[14] Williams D E G 1973 *J. Phys. F: Met. Phys.* **3** 1898
[15] Baranov N V, Yermakov A A, Markin P E, Possokhov U M, Michor H, Weingartner B, Hilscher B and Kotur B 2001 *J. Alloys Compounds* **329** 22–30